ELSEVIER

Chemical Engineering Journal 138 (2008) 517–522

Chemical Engineering Journal

www.elsevier.com/locate/cej

Preparation of Pd–B/TiO_2 amorphous alloy catalysts and their performance on liquid-phase hydrogenation of *p*-nitrophenol

Zhenye Ma, Lixiong Zhang, Rizhi Chen, Weihong Xing, Nanping Xu *

College of Chemistry and Chemical Engineering, Nanjing University of Technology, Nanjing 210009, PR China

Received 16 April 2007; received in revised form 30 June 2007; accepted 6 July 2007

Abstract

The Pd–B/TiO_2 amorphous alloy catalyst were prepared by the liquid-phase chemical reduction with KBH_4 aqueous solution. The catalysts were characterized by X-ray diffraction (XRD), X-ray photoelectron spectroscopy (XPS), differential scanning calorimetry (DSC) and high reaction transmission electron microscopy (HRTEM). Analysis results show that the active metal clusters Pd–B are homogeneously dispersed on the surface of the TiO_2 particles and the size of most metal clusters is below 10 nm. The as-prepared Pd–B/TiO_2 catalysts exhibit higher catalytic properties (activity, selectivity, and stability) than the corresponding Pd-based catalysts and Ni-based catalysts during the liquid-phase *p*-nitrophenol (PNP) hydrogenation to *p*-aminophenol (PAP), which indicates the promoting effect of the alloying B and TiO_2 support. Enriched electron state of Pd active sites and high dispersion of the Pd–B active sites on TiO_2 support are mainly attributed to the improvement of catalytic activity of Pd–B/TiO_2 amorphous alloy catalyst. The effects of different reaction parameters such as support, pH value, Pd loading and the thermal treatment on the catalytic activity of the Pd–B/TiO_2 amorphous alloy catalyst were studied in detail. The maximum preparation condition is achieved by using TiO_2 (P25), pH 12 and 0.5% amount of Pd loading.

Keywords: Pd–B/TiO_2; Amorphous alloy; Hydrogenation; *p*-Nitrophenol; *p*-Aminophenol

1. Introduction

p-Aminophenol (PAP) is an important intermediate for the manufacture of analgesic and antipyretic drugs such as paracetamol, acetanilide, phenacetin, and so forth [1–4]. The direct catalytic hydrogenation of *p*-nitrophenol (PNP) is considered as an efficient and greener route for the preparation of PAP [1]. Raney Ni [5], nano-sized Ni [6] and several precious metals such as Pd/C [1] have been selected as catalysts for this reaction.

In recent years, metal–metalloid amorphous alloy catalysts have attracted much attention owing to their excellent activity and selectivity as well as their strong sulfur resistance in various hydrogenation reactions [7–13]. Amorphous alloys belong to a class of material with long-range disordered but short-range ordered structure. Their single-phase character and the absence of surface segregation of the alloying elements ensure that the active sites are in a uniform dispersion in a homogenous chemical environment. They also have a high concentration of highly unsaturated coordinative sites, which makes adsorption and surface reactions easier [11]. Although a lot of amorphous alloy catalysts were reported such as Ni (Co, Fe)–B (P, C) amorphous alloy, few Pd-based amorphous catalysts have been reported so far. One of the most important reasons is that the thermal stability of these Pd-based amorphous alloy catalysts is very poor and the crystallization process will occur easily during the reaction even at very low temperature. It is reported that the amorphous structure could be greatly stabilized by depositing the ultrafine alloy particles on a suitable support [12].

Therefore, in this paper, we reported a novel Pd–B/TiO_2 amorphous catalyst which exhibited excellent activity during the hydrogenation of PNP for the preparation of PAP. Pd–B/TiO_2 amorphous catalysts were prepared by liquid-phase chemical reduction and the properties were characterized by XRD, XPS, DSC and HRTEM. Attention was chiefly paid to the catalytic properties investigation of Pd–B/TiO_2 in the PNP hydrogenation in comparison with the corresponding Pd/TiO_2, crystallized Pd–B/TiO_2, unsupported Pd–B, commercial Pd/C catalysts, nano-sized Ni and Raney Ni. The effects of the preparation parameters on the activity of the Pd–B/TiO_2 amorphous alloy catalyst were also investigated.

* Corresponding author. Tel.: +86 25 83587171; fax: +86 25 83300345.
E-mail address: mzynjust@163.com (N. Xu).

1385-8947/$ – see front matter © 2007 Elsevier B.V. All rights reserved.
doi:10.1016/j.cej.2007.07.028

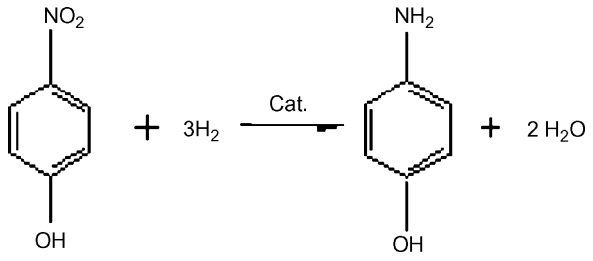

Scheme 1. Catalytic hydrogenation of *p*-nitrophenol to *p*-aminophenol.

2. Experimental

2.1. Catalyst preparation

The Pd–B/TiO_2 catalysts were prepared by liquid-phase chemical reduction method as follows. TiO_2 powder was impregnated with dilute $PdCl_2$ solution. After 20 min ultrasonic vibration and further 1-h stirring in order to get a well-dispersed sample, the obtained suspension was reduced by adding dropwise the aqueous solution of KBH_4 under the vacuum condition. Excess KBH_4 (molar ratio of KBH_4 to Pd is 10:1) was used to ensure the complete reduction of Pd^{2+} ions. The reaction mixture was stirred until no significant bubbles were observed. Then the resulting suspension was washed thoroughly with distilled water and subsequently with 99.9% alcohol (EtOH). The as-prepared Pd–B/TiO_2 catalyst was stored in a certain amount of EtOH to protect it from oxidation. The Pd-loading of the catalyst was adjusted by changing the amount of $PdCl_2$ in the solution for impregnation.

Unsupported Pd–B was prepared according to the above method without addition of TiO_2 support. The Pd/TiO_2 catalysts were prepared also according to the above method, but $N_2H_4{\cdot}H_2O$ was used as the reduction agent at 80 °C.

2.2. Catalytic hydrogenation of PNP

The simplified schematic diagram of hydrogenation of *p*-nitrophenol is shown in Scheme 1.

The catalytic hydrogenation of *p*-nitrophenol to *p*-aminophenol was performed in a 300 ml stainless steel autoclave with electromagnetic stirrer and temperature control unit. The operation conditions of catalytic *p*-nitrophenol reduction are listed in Table 1. The reactor was heated to a desired temperature under slow stirring (100 rpm). After the temperature equilibrated at the set point, hydrogen gas was introduced to a set pressure and the system was stirred vigorously (300 rpm). At the end of the reaction, the reactor was cooled to the ambient temperature and samples were taken from the reaction system. The solid catalyst was immediately separated from the aqueous phase by centrifugation and the remaining top solution was analyzed by a HPLC (Agilent 1100 Series, USA) equipped with a diode array detector (DAD) and an auto-sampler.

Table 1
The operation conditions of catalytic hydrogenation of *p*-nitrophenol

Reaction temperature (K)	375
Operating pressure (bar)	16.5
Volume of ethanol (ml)	143
Volume of water (ml)	20
Amount of *p*-nitrophenol (g)	14
Amount of catalytic (g)	0.3
Stirring rate (rpm)	300

2.3. Catalyst characterization

The amorphous characters of the as-prepared samples were determined by X-ray diffraction (XRD) performed on a Bruker D8 Advance instrument using Cu Kα radiation (λ = 0.154178 nm) from 5° to 90° (in 2θ) with the scanning rate of 2.4°/min.

The surface electronic states were determined by X-ray photoelectron spectroscopy (XPS) performed using PHI 5300 ESCA instrument. The analysis chamber was operated under ultrahigh vacuum with a pressure close to 10^{-7} Pa. X-rays were produced by a monochromatized magnesium anode (Mg Kα, 1253.6 eV). All binding energy values were calibrated by using the value of contaminant carbon (C1s = 284.6 eV) as a reference.

The crystallization process was followed by differential scanning calorimetry (DSC) under N_2 atmosphere at a heating rate of 10 K min^{-1} carried out by Diamond DSC instrument. The micrograph of the Pd–B amorphous alloy was determined by high reaction transmission electron microscopy (HRTEM) carried out on a JEOL TEM-2100 transmission electron microscope. The samples were dropped onto the surface of carbon membrane and dried at ambient conditions.

3. Results and discussion

3.1. Performance of Pd–B/TiO_2 catalyst

3.1.1. Effect of support

Pd–B amorphous alloy loaded on three different TiO_2 supports (A, B and C) with the same Pd loading amount of 2 wt.% was studied. The characteristics of the three different supports are listed in Table 2, and the catalytic activity results are displayed in Fig. 1. As can be seen, the Pd–B/TiO_2 catalyst exhibits the highest activity by using support A (P25). This suggests that the higher specific surface area and smaller size of P25 might play a very important role in catalytic performance. Therefore, selecting a suitable catalyst support is essential for the synthesis of *p*-aminophenol from *p*-nitrophenol. Consequently, TiO_2 (P25) was chosen as the support of Pd–B active components in this work.

Table 2
The characteristics of three different TiO_2 supports

Support	Crystal composition	Surface area (m^2/g)	Particle size (nm)
A (P25)	79% Anatase + 21% rutile	49.796	21
B	Anatase	42.547	40
C	Anatase	10.057	240

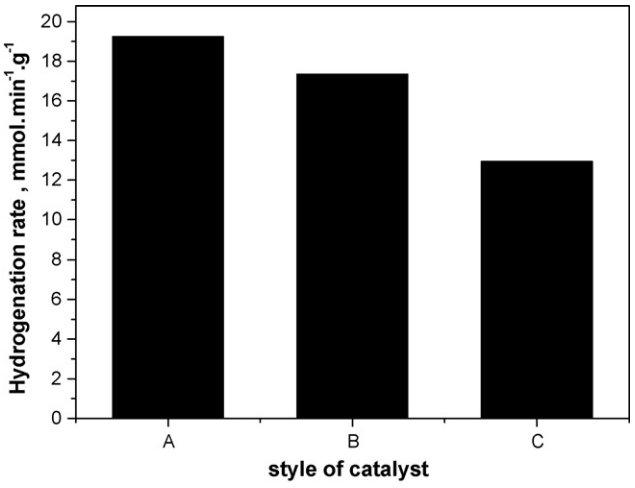

Fig. 1. Effect of support on the catalytic activity of Pd–B/TiO_2 amorphous catalyst.

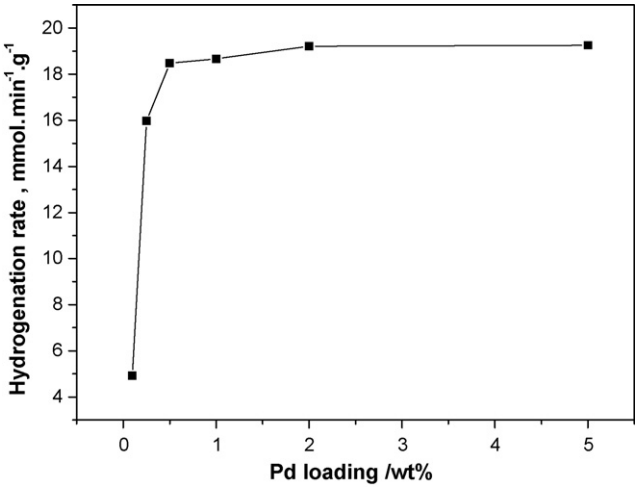

Fig. 3. Effect of Pd-loading on the catalytic activity of Pd–B/TiO_2 amorphous catalyst.

3.1.2. *Effect of pH value*

It has been pointed out that the pH value of metal salt solution is an important parameter to influence the structure of catalyst [14,15]. To investigate the pH value effect on the catalytic activity of the Pd–B/TiO_2 catalyst, a series of catalysts were prepared by controlling the pH value of solution at 3, 5, 7, 10, 12, 13, and catalytic experiments were carried out respectively. The results are displayed in Fig. 2. As shown in Fig. 2, the catalytic activity of Pd–B/TiO_2 is distinctly affected by the pH value. With the increase of pH value, the catalytic activity first decreases and then increases. The catalysts prepared at acid or basic solution display higher catalytic activity. While the catalyst prepared by controlling the pH value at 7 shows the lower catalytic activity. This is attributed to the dispersion of support TiO_2 at different pH value. There exists an amphoteric group named "titanol" (TiOH) on the surface of TiO_2, which undergoes acid–base equilibrium [16].

$$TiOH + H^+ \rightleftarrows TiOH_2^+ \qquad pH < 6.25 \tag{1}$$

$$TiOH \rightleftarrows TiO^- + H^+ \qquad pH > 6.25 \tag{2}$$

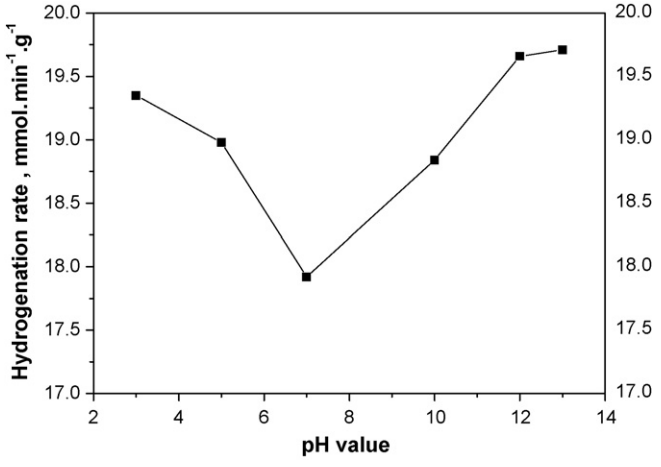

Fig. 2. Effect of pH value on the catalytic activity of the Pd–B/TiO_2 amorphous catalyst.

The stable properties can be greatly changed under different pH value. If the pH value of solution is higher or lower than the identical electric point (IEP = 6.25) of TiO_2, the surface of TiO_2 will be negatively or positively charged, respectively. The further the pH value of solution is from the IEP of TiO_2, the more stable and the better dispersed TiO_2 particles will be. Conversely, if the pH value of the solution is close to the identical electric point, TiO_2 particles will aggregate.

3.1.3. *Effect of Pd loading*

To obtain the maximum activity of the Pd–B/TiO_2 catalyst, the effect of the Pd-loading on catalytic activity was also investigated. The results are illustrated in Fig. 3. The Pd loading shows a significant effect on the catalytic activity of the Pd–B/TiO_2 catalyst. The activity of Pd–B/TiO_2 catalyst changes with the increase of the amount of Pd loading at three different stages. The activity increases sharply with the increase of Pd loading from 0.1 to 0.5 wt.% and increases slowly with the increase of Pd loading from 0.5 to 2 wt.%. This is attributed to the increase in the number of the catalytic active sites with increasing loading. The activity remains nearly constant with the further increase of Pd loading from 2 to 5 wt.%. The aggregation of Pd–B leads to the dispersion of active sites to decrease at Pd contents above 2 wt.%.

This suggests that active atomic arrangement and active particle size on the surface of catalyst may have a great influence on the catalytic activity. In order to further observe the morphology of Pd–B catalyst, HRTEM of the catalyst (2 wt.%) was taken and one typical photograph is shown in Fig. 4. Small particles represent clusters of the active metal and large particles represent TiO_2 particles. As shown in Fig. 4, the active metal clusters are clearly visible and are homogeneously dispersed on the TiO_2 particles. The size of most metal clusters is below 10 nm.

3.1.4. *Effect of the thermal treatment*

The influence of the amorphous structure of the Pd–B on its hydrogenation activity can be further confirmed by observing

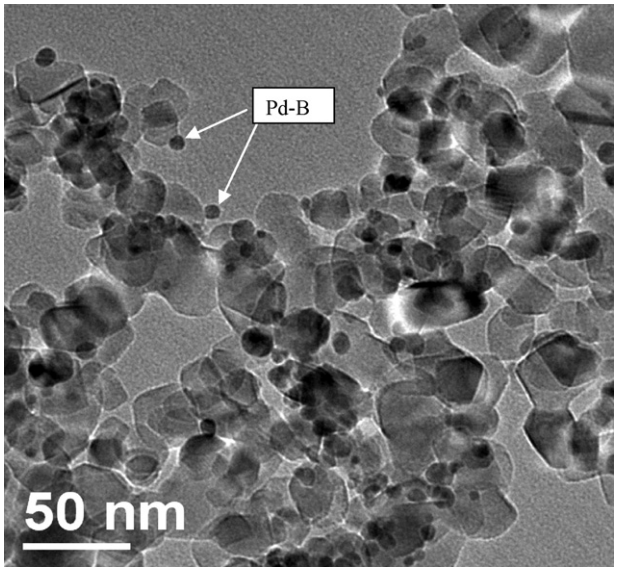

Fig. 4. HRTEM image of Pd–B/TiO_2 amorphous alloy catalyst.

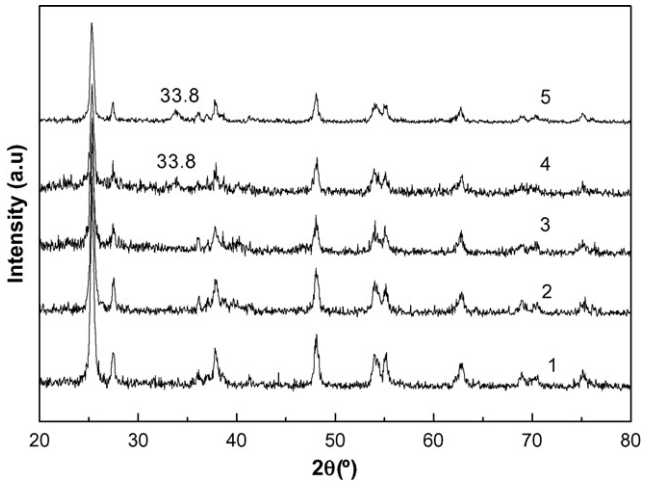

Fig. 6. X-ray diffraction patterns of samples. (1) TiO_2; (2) Fresh Pd-B/TiO_2; (3) Pd-B/TiO_2 (heated at 200 °C for 2 h); (4) Pd-B/TiO_2 (heated at 300 °C for 2 h); (5) Pd-B/TiO_2 (heated at 400 °C for 2 h).

the change in the activity of Pd–B/TiO_2 catalyst during its thermal treatment. The as-prepared Pd–B/TiO_2 catalyst was heated at 200, 300 and 400 °C for 2 h under Ar atmosphere, respectively, and the results are displayed in Fig. 5. As can be seen, under the same given reaction conditions, fresh Pd–B/TiO_2 and Pd–B/TiO_2 heated at 200 °C, have the higher catalytic activities than the Pd–B/TiO_2 heated at 300 °C and 400 °C. The effect of thermal treatment is much evident for the hydrogenation of *p*-nitrophenol.

Fig. 6 shows the XRD patterns of the Pd–B/TiO_2 sample treated at 200, 300 °C and 400 °C in Ar flow for 2 h, respectively. Although various crystalline diffractional peaks, mainly corresponding to crystalline TiO_2 are observed, there is no significant change in the XRD patterns when the sample was heated at 200 °C for 2 h. Abrupt crystallization of the Pd–B amorphous alloy is observed as a diffractional peak around $2\theta = 33.8°$ assigned as the Pd_2B alloy phase appears when the sample was treated at a temperature higher than 300 °C. It can be concluded that crystallization temperature of the Pd–B amorphous alloy is between 200 and 300 °C. The crystallization of the Pd–B amorphous alloy may be the main reason which leads to the activity decrease of catalyst heated at higher temperature.

The crystallization process of the Pd–B amorphous alloy can be also followed by the DSC spectrum (see Fig. 7). It can be seen that the supported Pd–B amorphous alloy exhibits an exothermic peak at 278.2 °C, indicating that the amorphous structure is thermodynamically metastable and the crystallization of the Pd–B amorphous alloy occurs spontaneously at 278.2 °C. However, the crystallization temperature of the Pd–B/TiO_2 catalyst is 40 °C higher than that of the unsupported Pd–B catalyst, indicating a very strong stabilizing effect of TiO_2 support on the Pd–B amorphous structure. Such a stabilizing effect can be mainly attributed to the dispersion of the Pd–B alloy particles on the

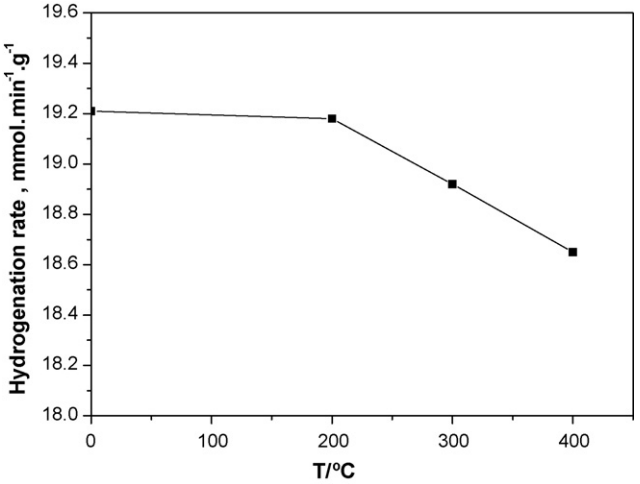

Fig. 5. Effect of treatment temperature on the catalytic activity of Pd–B/TiO_2 amorphous catalyst.

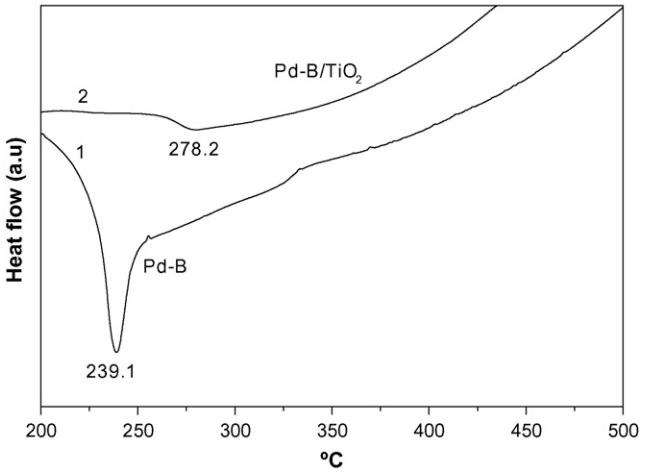

Fig. 7. DSC curves of (1) unsupported Pd–B and (2) Pd–B/TiO_2 amorphous alloy catalyst.

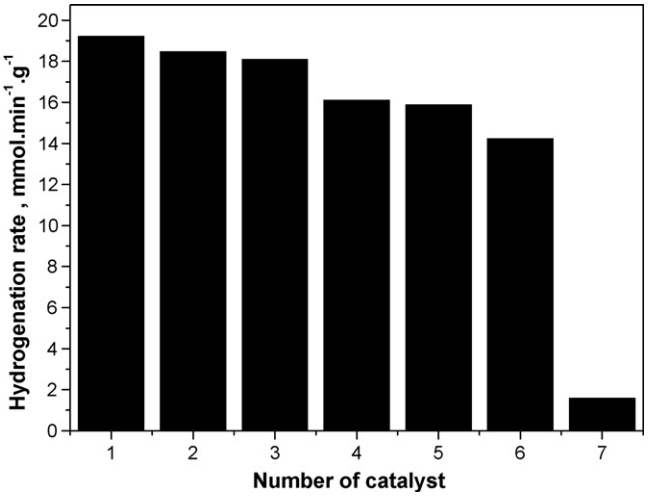

Fig. 8. Catalytic activity of *p*-nitrophenol hydrogenation over different catalysts at the same conditions. (1) 2% Pd–B/TiO_2; (2) 0.5% Pd–B/TiO_2; (3) 2% Pd/C; (4) nanosized Ni; (5) 2% Pd /TiO_2; (6) Pd–B; (7) Raney Ni.

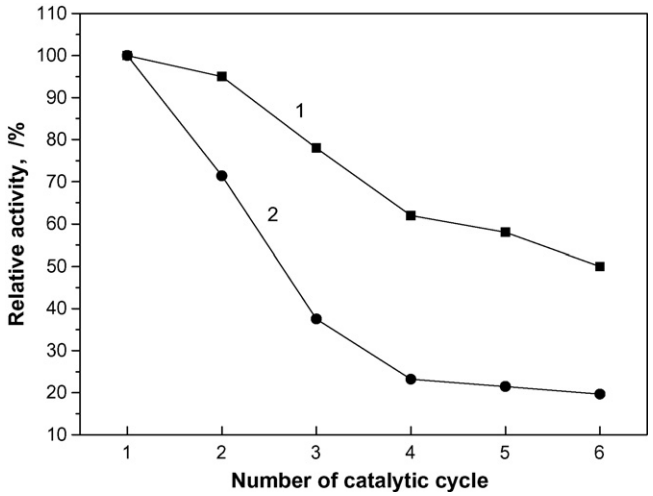

Fig. 9. Catalytic stability investigations of Pd–B/TiO_2 and Raney Ni.

support and the strong interaction between Pd–B alloy and the support.

3.2. Comparative catalytic activity with other catalysts

The catalytic activity of as-prepared Pd–B/TiO_2 amorphous catalyst was compared with Pd-based catalysts (such as the corresponding crystallized Pd–B/TiO_2 catalyst, the Pd/TiO_2 catalyst obtained by N_2H_4 H_2O reduction, unsupported Pd–B, and the commercial Pd/C catalyst) and Ni-based catalysts (nano-sized Ni and Raney Ni). The results are shown in Fig. 8. As shown in Fig. 8, the catalytic activity sequence is Pd–B/TiO_2 (2%) ≈ Pd–B/TiO_2 (0.5%) ≈ Pd/C (2%) > Pd/TiO_2 ≈ nano-sized Ni > Pd–B>Raney Ni. Pd–B/TiO_2 amorphous alloy shows the highest catalytic activity. *p*-Aminophenol is found to be the only product for all catalysts except Raney Ni in the activity tests, implying that the selectivity is almost 100%, while there is an impurity peak in the HPLC analysis of the reaction products catalyzed by Raney Ni. The impurity might be the product of benzene ring hydrogenation, perhaps caused by the micropores of Raney Ni [17].

In order to explain the better catalytic activity of the amorphous Pd–B/TiO_2 alloy, the surface electronic states were measured by XPS. Only metallic Pd species in the Pd–B alloy are observed, corresponding to the two peaks with the binding energies around 334.3 eV ($Pd3d_{5/2}$) and 339.5 eV ($Pd3d_{3/2}$). The peak around 188.5 eV corresponds to the B species alloying with Pd. In comparison with the binding energy of pure Pd (335.0 eV corresponding to $Pd3d_{5/2}$) and pure B (187.2–187.5 eV corresponding to B_{1s}), the binding energy of metallic Pd in the Pd–B alloy shifts negatively about 0.7 eV, while that of the B in the Pd–B alloy shifts positively about 1.0 eV. Therefore, some electrons transferred from B to Pd in the Pd–B alloy, making Pd electron enriched. Therefore, we suggest the reason for higher catalytic activity of Pd–B/TiO_2 is a combination effect of enriched Pd electronic states, smaller particle size of Pd–B and better dispersion of Pd–B on the support.

3.3. The activity stability of Pd–B/TiO_2 catalyst

The activity stability of Pd–B/TiO_2 catalysts was compared with Raney Ni. The correlations between the relative degree of catalyst deactivation and the number of catalytic reaction cycles are shown in Fig. 9. During each continuous *p*-nitrophenol hydrogenation cycle, both Pd–B/TiO_2 and Raney Ni are undergoing deactivation. Throughout six continuous hydrogenation cycles, the Pd–B/TiO_2 system suffers 42% deactivation, while the Raney nickel system suffers 80% deactivation. These results indicate that the catalytic stability of Pd–B/TiO_2 catalyst is superior to that of the Raney Ni.

4. Conclusions

Amorphous Pd–B/TiO_2 alloy catalysts were prepared by the liquid-phase chemical reduction at ambient temperature. The best conversion of PNP were obtained over the TiO_2 support (P25 type), with the Pd loading of 0.5 wt.% and pH 12. The as-prepared Pd–B/TiO_2 amorphous catalyst exhibited much higher catalytic properties (activity, selectivity, and stability) than other Pd-based catalysts and Ni-based catalysts. The promoting effect of alloying B was mainly attributed to the formation of the amorphous structure and the modification of the surface electronic state of Pd active sites, while the promoting effect of TiO_2 support was ascribed to its high dispersion of the Pd active sites and its stabilization of the amorphous structure. Enriched electron state of Pd active sites and high dispersion of the Pd–B active sites on TiO_2 support are mainly attributed to the improvement of catalytic performance of Pd–B/TiO_2 amorphous alloy catalyst.

Acknowledgements

This work was financially supported by the State Key Development Program for Basic Research of China (2003CB615702); the Major Program of National Natural Science Foundation of China (20436030). The National Key Technologies R&D

Program (2004BA310A3); Jiangsu Planned Projects for Post-doctoral Research Funds (0501021C).

References

[1] M.J. Vaidya, S.M. Kulkarni, R.V. Chaudhari, Org. Process Res. Dev. 7 (2003) 202–208.
[2] C.V. Rode, M.J. Vaidya, R. Jaganathan, R.V. Chaudhari, Chem. Eng. Sci. 56 (2001) 1299–1304.
[3] L.T. Lee, M.H. Chen, C.N. Yao, US patent 4,885,389 (1989) to Industrial Technology Research Institute (TW).
[4] R.V. Chaudhari, S.S. Divekar, M.J. Vaidya, C.V. Rode, US patent 6,028,227 (2000) to Council of Scientific & Industrial Research (New Delhi, India).
[5] R.Z. Chen, Y. Du, C.L. Chen, W.H. Xing, N.P. Xu, C.X. Chen, Z.L. Zhang, Huagong Xuebao 54 (2003) 704–707 (in Chinese).
[6] Y. Du, H.L. Chen, R.Z. Chen, N.P. Xu, Appl. Catal. A: Gen. 277 (2004) 259–264.
[7] M.H. Wang, H.X. LI, Y.D. WU, J. Zhang, Mater. Lett. 57 (2003) 2954–2964.
[8] Y.J. Hou, Y.Q. Wang, F. He, S. Han, Z.T. Mi, W. Wu, Mater. Lett. 58 (2004) 1267–1271.
[9] H. Li, H.X. Li, J.F. Deng, Catal. Today 74 (2002) 53–63.
[10] J.F. Deng, H.X. Li, W.J. Wang, Catal. Today 51 (1999) 113–125.
[11] R.B. Zhang, F.Y. Li, N. Zhang, O.J. Shi, Appl. Catal. A: Gen. 239 (2003) 17–23.
[12] X.B. Yu, M.H. Wang, H.X. Li, J. Chem. Eng. Chin. Univ. 20 (2006) 476–480.
[13] X.J. Luo, X.H. Yan, J.Q. Sun, W.J. Wang, J.F. Yang, Appl. Catal. A: Gen. 202 (2000) 17–23.
[14] S. Linderoth, S. Morup, J. Appl. Phys. 67 (1990) 4472–4476.
[15] F.X. Zhang, J.X. Chen, X. Zhang, W.L. Gao, R.C. Jin, N.J. Guan, Catal. Today 93 (2004) 645–650.
[16] C. Kormann, D.W. Bahnemann, M.R. Hoffmann, Environ. Sci. Technol. 25 (1991) 494–498.
[17] D.H. Zuo, Z.K. Zhang, Z.L. Cui, Chin. J. Mol. Catal. 9 (1995) 298–302.